JOURNAL OF APPLIED ELECTROCHEMISTRY 12 (1982) 425–434

*Catalytic electrodes for the Redox Flow Cell energy storage device**

C. Y. YANG

Department of Energy and Environment, Brookhaven National Laboratory, Upton, New York 11973, USA

Received 28 July 1981

Several porous electrode materials have been studied for the redox couple Cr^{3+}/Cr^{2+}. The electrochemically active surface area, the hydrogen evolution overpotential and the limiting current of the chromium redox reactions were measured. Useful kinetic parameters can be deduced although their accuracies are limited due to the porous nature of the materials studied. The results presented will primarily be for one kind of graphite material and for ZrC. The performance of the ZrC electrode is promising and exhibits a significant improvement over carbon electrodes. The effects of lead chloride as a catalytic additive to the solution have been studied. Finally, the correlation between electrode performance and chromium complex formation will be discussed since the bridging mechanism is important in the Cr^{3+}/Cr^{2+} redox reaction.

1. Introduction

The Redox Flow Cell is an electrochemical device for bulk energy storage, such as power station load levelling. It was first developed by Thaller [1] and others at the NASA Lewis Research Center. Two redox couples, such as Fe^{3+}/Fe^{2+} and Cr^{3+}/Cr^{2+}, are separated by an ion-selective membrane in the cell. External energy can be stored by electrochemically oxidizing one redox couple (e.g. Fe^{3+}/Fe^{2+}) and reducing the other (e.g. Cr^{3+}/Cr^{2+}). Stored energy can then be released upon demand by reversing the redox operation.

A Redox Flow Cell based on the two redox couples Fe^{3+}/Fe^{2+} and Cr^{3+}/Cr^{2+} has a reasonably high open circuit potential (theoretical value ~ 1.1 V). However, the chromium half-cell redox reaction rate at an ordinary electrode such as carbon is several orders of magnitude slower than the iron half-cell redox reaction on an electrode of the same material. Furthermore, hydrogen evolution is a competing reaction at the chromium electrode since the standard potential of Cr^{3+}/Cr^{2+} is -0.41 V (RHE). Therefore, electrodes with selective activity, namely, high hydrogen overpotential and reversible chromium redox reaction, are needed.

This study deals primarily with electrode improvements for the Cr^{3+}/Cr^{2+} redox couple. The results presented here include the evaluation procedures of different electrode materials, the effects of catalytic additives to the electrolyte and any possible ion complex formation.

2. Experimental procedures

The ZrC samples examined in this report were obtained from Los Alamos Scientific Laboratory. Their electrical conductivity is fairly high and comparable to that of graphite. Carbon fibre tubes were used as starting materials and the production procedures involved: (a) chemical vapour deposition, (b) densification, (c) heat treatment [2]. The stoichiometry and density of the products can be conveniently controlled. The samples used in this study were approximately 1 : 1 Zr : C with a low density (70% porosity). Three kinds of porous graphite electrodes have been studied. According to their forms and manufacturers, they were: (a) Union Carbide WCA cloth, (b) Union Carbide felt, and (c) Hitco G 2252 cloth. Basically, they all exhibited similar characteristics except for specific surface areas. (The surface area measurements will

*Work performed under the auspices of the US Department of Energy under Contract No. DE-AC02-76CH00016.

0021-891X/82/040425-10$03.70/0

be discussed below.) However, the hydrogen evolution overpotential of the felt is about 100–200 mV anodic to that of the cloths. In the following only the results of the Hitco cloth will be discussed and it is taken as a reference for comparison with other electrode materials.

Electrochemical measurements were made with a Wenking 70 TSI potentiostat. This unit was programmed with either a Wenking SMP72 or Interstate F74 function generator. An Esterline Angus 530 *X–Y* recorder and a Nicolet Explorer II digital storage oscilloscope were used as recording devices. The X-ray photoemission spectra (XPS) were obtained with a DuPont 650 B electron spectrometer.

3. Results and discussion

3.1. *Carbon electrodes and zirconium carbide electrodes*

Figure 1 shows typical cyclic voltammograms of a Hitco cloth. As can be seen in Fig. 1a, significant hydrogen evolution starts at about − 0.7 V (SCE). In Fig. 1b, the increased cathodic current indicates a contribution from the reduction of Cr^{3+} to Cr^{2+}, and the anodic peak at 0.05 V (SCE) corresponds to the oxidation of Cr^{2+} to Cr^{3+}. Decreasing the sweep rate shifts the anodic peak position in the negative direction (the standard potention of $Cr^{3+} + e \rightleftarrows Cr^{2+}$ is about − 0.65 V vs SCE). However, the Cr^{3+} reduction peak was still buried under the H_2 evolution current and these two cathodic contributions could not be resolved.

The ZrC samples in the state they were received from the manufacturer were no better than the graphite cloth as electrodes for Cr^{3+} reduction. It was found that samples soaked in 1 mol dm^{-3} HCl and held at a cathodic potential between − 0.6 and − 0.8 V (SCE) for an extended period of time (several hours) became more active. The discussion of the activation of ZrC will be presented later. Qualitatively, the cyclic voltammetric behaviour of an activated ZrC sample is very similar to that of the carbon electrode shown in Fig. 1. However, quantitatively the activated ZrC sample showed a much greater current density (threefold), higher hydrogen evolution overpotential (by 50 mV) and lower Cr^{3+} reduction overpotential (by 80 mV) at the same sweep rate of 280 mV s^{-1}. This can be considered as evidence that the activated ZrC electrode has a better activity and the desired selectivity for the Cr^{3+}/Cr^{2+} redox reaction.

3.2. *Electrochemically active surface area*

Because of the porous nature of the materials studied here, the observed difference in activity

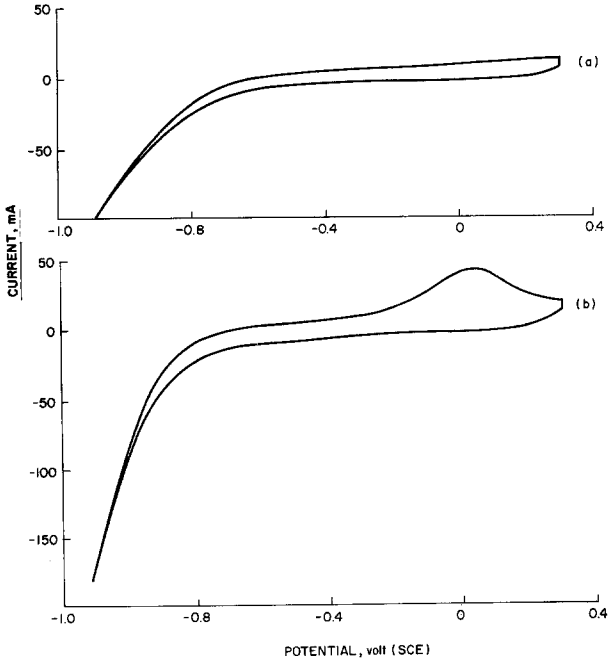

Fig. 1. Cyclic voltammograms of a graphite cloth electrode with a sweep rate of 280 mV s^{-1}. Sample area 2 cm × 2 cm; (a) 1 mol dm^{-3} HCl; (b) 1 mol dm^{-3} HCl + 0.005 mol dm^{-3} Cr^{3+}.

may be due to the difference in their electrochemically active surface areas. In order to distinguish kinetic effects from surface area effects two methods were used to estimate the electrochemically active surface area; these involved measuring the double-layer capacitance in the supporting electrolyte.

The first method is to use cyclic voltammetry in the non-Faradaic region [3], i.e. the region where no electrochemical reactions are taking place (e.g. − 0.5 to 0.1 V vs SCE). It was estimated that the capacitance is 1.1×10^3 μF cm^{-2} for the carbon cloth and 6.3×10^3 μF cm^{-2} for the ZrC electrode.

Another method is to apply an incremental potential step to the electrode in the non-Faradiac region [4]. The measured values are $0.7 \times 10^3 \mu$F cm^{-2} for the carbon cloth and 4.7×10^3 μF cm^{-2} for the ZrC electrode, respectively. The difference between the two methods is less than 30% and both methods showed that the double-layer capacitance of ZrC is about six times that of Hitco cloth.

The measured double-layer capacitances for a smooth graphite electrode [5, 6] are 3 μF cm^{-2} for a basal plane and 60 μF cm^{-2} for an edge plane. Since the exposed faces of the graphite cloth in this study were mainly edge planes (determined by the manufacturers), one can estimate the electrochemically active surface area of Hitco cloth to be around 15 times its apparent geometric area. No capacitance data on non-porous ZrC is available for comparison.

3.3. *Reversibility of ZrC electrodes*

Figure 2 shows linear sweep voltammograms of activated ZrC (Fig. 2a) and Hitco cloth (Fig. 2b) in solutions of different Cr^{3+} concentrations. The sweep rate was 0.5 mV s^{-1}, and the solution was stirred slowly with a magnetic bar at a rotation rate of 60 rpm to provide some mass transport. As can be seen, the reduction of Cr^{3+} on ZrC not only starts at a more positive value than on graphite cloth, but it also reaches a limiting current region without significant H_2 evolution. Similar measurements for more concentrated solutions have been performed, and the limiting current (at a fixed stirring rate) increased in proportion to the Cr^{3+} concentration up to 0.5 mol dm^{-3}.

Figure 3 is a series of cyclic voltammograms of an activated ZrC electrode with different sweep rates. It can be seen that the cathodic current contributions from H_2 evolution and Cr^{3+} reduction are resolved with decreasing sweep rates. No similar behaviour was observed for carbon cloth electrodes. This provides further evidence that the Cr^{3+}/Cr^{2+} reduction is relatively more reversible

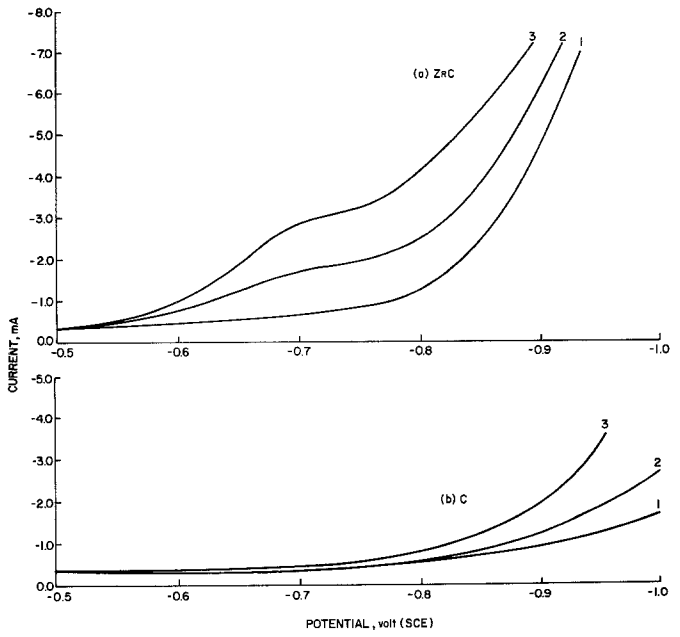

Fig. 2. Linear sweep voltammograms of (a) an activated ZrC electrode; (b) a graphite cloth electrode with a sweep rate of 0.5 mV s^{-1}. Curve 1, 1 mol dm^{-3} HCl; curve 2, 1 mol dm^{-3} HCl + 0.005 mol dm^{-3} Cr^{3+}; curve 3, 1 mol dm^{-3} HCl + 0.01 mol dm^{-3} Cr^{3+}.

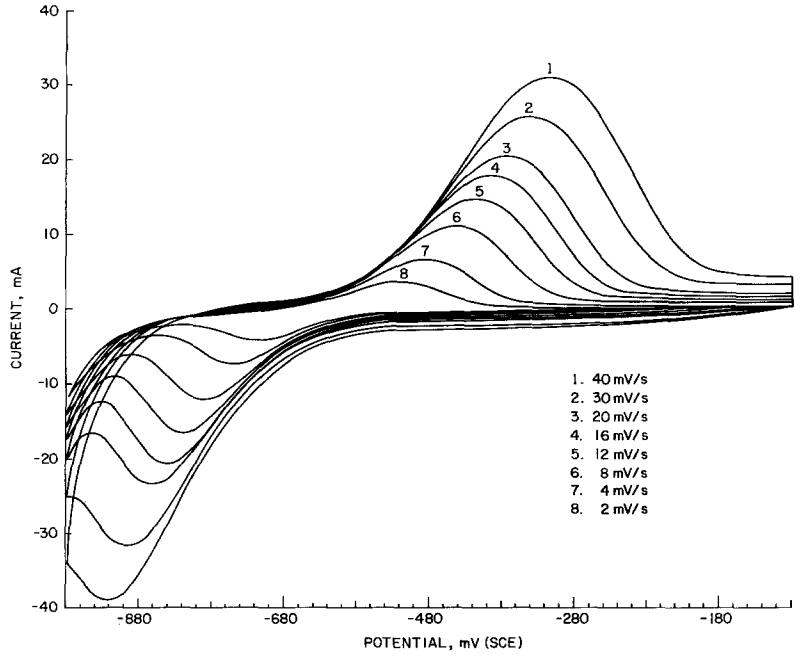

Fig. 3. A series of cyclic voltammograms of an activated ZrC electrode with different sweep rates. Electrolyte, 1 mol dm^{-3} HCl + 0.005 mol dm^{-3} Cr^{3+}.

on ZrC than carbon. For an electrode process involving a single electron transfer step, the peak current of voltammetric sweep is [7, 8]

$$i_p = 3.01 \times 10^5 \, n^{3/2} \, \alpha^{1/2} \, D^{1/2} \, C^0 \, S^{1/2} f A \quad (1)$$

where n is the number of electrons transferred, α is the transfer coefficient, D is the diffusivity, C^0 is the bulk concentration, S is the sweep rate, A is the geometric electrode area and f is the surface area factor. A plot of the cathodic i_p versus $S^{1/2}$ is shown in Fig. 4 and is a straight line.

The corresponding peak potential is given by [7, 8]

$$E_p = E_{1/2} - b[0.52 - 1/2 \log (b/D) - \log k_s + 1/2 \log S] \quad (2)$$

where $E_{1/2}$ is the polarographic half-wave potential, k_s is the standard rate constant and b is the Tafel slope. A plot of $\log S$ versus E_p of the cathodic branch is shown in Fig. 5. The linearity is obeyed up to a sweep rate of 8 mV s^{-1}. At very slow sweep rates, the electrode reactions exhibit reversible behaviour, i.e. E_p is independent of sweep rate [7, 8].

$$E_p = E_{1/2} - 1.1 \frac{RT}{nF}. \quad (3)$$

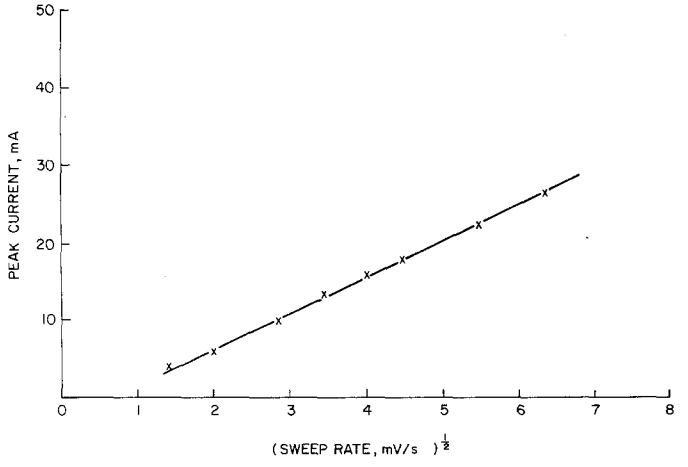

Fig. 4. Plot of the cathodic peak current (Fig. 3) versus square root of the sweep rate.

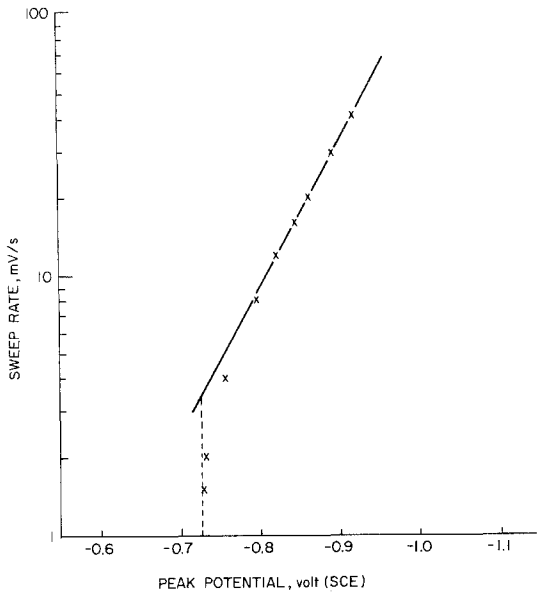

Fig. 5. Plot of the logarithmic sweep rate versus the cathodic peak potential (Fig. 3). The dotted line is extrapolated for slow sweep rates.

From the slope of the irreversible region (Equation 2), one can obtain the Tafel slope b. Also, from the critical sweep rate, S_c (where the solid line and dotted line intersect in Fig. 5), one can deduce the standard rate constant k_s by equating Equations 2 and 3, provided that D is known.

For the cathodic branch, one obtains $b = 175$ mV/decade (from Fig. 5) and $\alpha = 0.35$ ($\alpha = 2.3\,RT/bnF$). Assuming $D_{Cr^{3+}} \sim 6 \times 10^{-6}$ cm^2 s^{-1} [9] together with S_c measured from Fig. 5, one obtains $k_s \simeq 4.6 \times 10^{-4}$ cm s^{-1}. Substituting α, D and C^0 into Equation 1, one can deduce the surface area factor $f \simeq 12$ which is very close to that of Hitco graphite cloth derived by double-layer capacitance measurements. It suggests that the surface roughness effect is rather similar between graphite cloth and ZrC, and the difference in electrochemical behaviour is catalytic in nature. Similar estimates can be made for the anodic branch. However, the initial bulk solution contained predominantly Cr^{3+} and, therefore, C^0 for Cr^{2+} can only be approximated when the different equations are applied.

3.4. *Activation of ZrC*

It was mentioned previously that the ZrC samples were electrochemically reduced before they became active for Cr^{3+} reduction. Preliminary studies indicate that an oxide layer exists on the non-active samples. Therefore, one can activate ZrC by properly reducing the oxide layer.

Auger and XPS spectra were obtained for ZrC in order to determine the surface composition and valence states of the surface elements. The Auger spectra showed that non-active ZrC has a significantly stronger oxygen signal than active ZrC. This suggests that certain forms of oxide exist on the surface and it impedes the Cr^{3+} reduction.

Figure 6 shows XPS spectra of the Zr 3d electrons of non-active (Fig. 6a) and activated (Fig. 6b) ZrC. It is obvious that the valence state of zirconium is quite different in the two cases. There are four peaks for activated ZrC and three peaks for the non-active sample indicating that zircon-

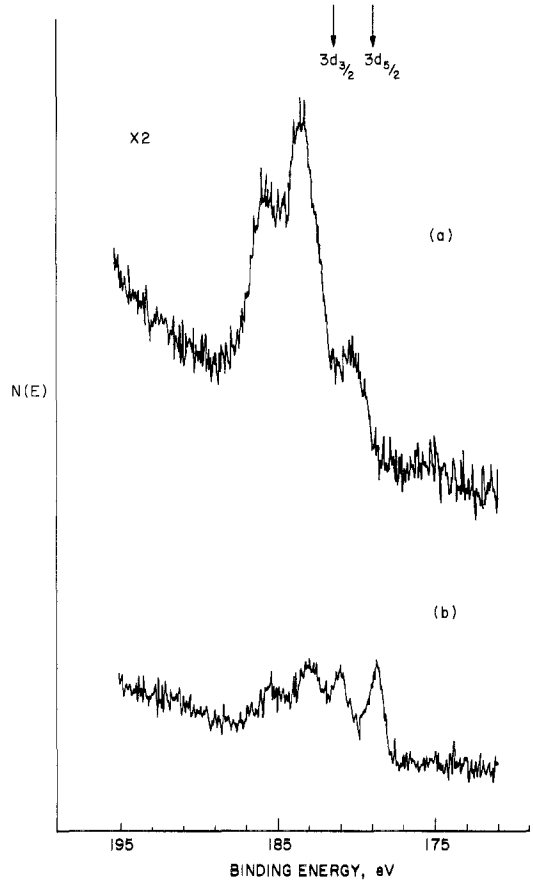

Fig. 6. XPS data of the Zr 3d electrons; (a) non-active ZrC electrode; (b) activated ZrC electrode. The arrows indicate the peak position of metallic zirconium.

ium is a more complicated, possibly multivalent, state in the former. The Zr 3d binding energies are, in general, smaller for the activated ZrC sample. This suggests a more reduced state for zirconium in the activated ZrC.

It was found also that the double-layer capacitance of ZrC increased after it was activated. Furthermore, one noticed a greater deviation from the ideal double-layer voltammetry behaviour for the non-active ZrC. Ideal double-layer behaviour should have an abrupt vertical current change when the potential sweep reverses direction in the non-Faradaic region. One can attribute deviation from this ideal behaviour to a resistive component in parallel with the double-layer capacitor. This is consistent with the suggestion that an oxide layer existed on the non-active ZrC surface, since oxide films are, in general, poor conductors. Further studies are needed in order to determine the structure and stoichiometry of the oxide. It is likely that this surface oxide will be different from ZrO_2, since the chemical bonding of zirconium in this material also involves carbon atoms.

3.5. *Catalytic additives*

Different additives to the solution have been tested for the Cr^{3+} reduction reaction by Giner and Cahill [10]. It has been found that adding $PbCl_2$ to the solution has desirable effects on the electrode, namely, high hydrogen overpotential and fast Cr^{3+} reduction. Further studies on the lead additive are reported below.

A small amout of $PbCl_2$ is soluble in acidic solution and dissociates into Pb^{2+} and Cl^-. During the reduction of Cr^{3+}, lead ions are also reduced and form layers of metallic lead on the electrode. The lead surface is responsible for the high hydrogen overpotential and fast Cr^{3+} reduction. However, during the oxidation of Cr^{2+}, lead dissolves back into the solution and the electrode activity is basically the same as the original substrate material.

Cyclic voltammetry studies of the effects of lead additives on a Hitco graphite cloth electrode are shown in Fig. 7. The dotted curve of Fig. 7a, which is similar to Fig. 1b, represents the voltammogram before the addition of $PbCl_2$. With the lead additives (solid curve in Fig. 7a), one notices that the cathodic peak is larger and has a potential closer to the standard potential of Cr^{3+}/Cr^{2+}.

The lead deposition current is buried in the reduction peak. However, the dissolution of lead is evidenced by the new anodic peak around -0.5 V (SCE). The Cr^{2+} oxidation peak is bigger than before and the peak potential is further away from the Cr^{3+}/Cr^{2+} standard potential. This is because in the cathodic cycle, a greater amount of Cr^{2+} ions have been produced near the surface due to the catalytic activity of lead. By decreasing the sweep rate (Fig. 7b), one is able to separate the two cathodic contributions due to Cr^{3+} reduction and

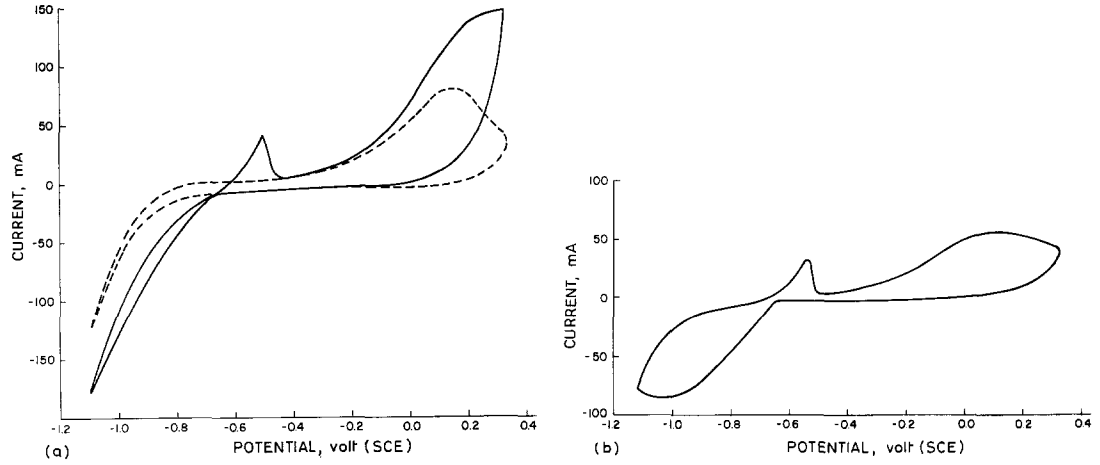

Fig. 7. The catalytic effects of lead additive on the Cr^{2+}/Cr^{3+} redox reaction on a graphite cloth electrode. Electrolyte 1 mol dm^{-3} HCl + 0.03 mol dm^{-3} Cr^{3+}; (a) dotted curve and solid curve corresponds to without and with 10^{-4} mol dm^{-3} Pb^{2+} additive, respectively; sweep rate 280 mV s^{-1}; (b) with 10^{-4} mol dm^{-3} Pb^{2+}, sweep rate 56 mV s^{-1}.

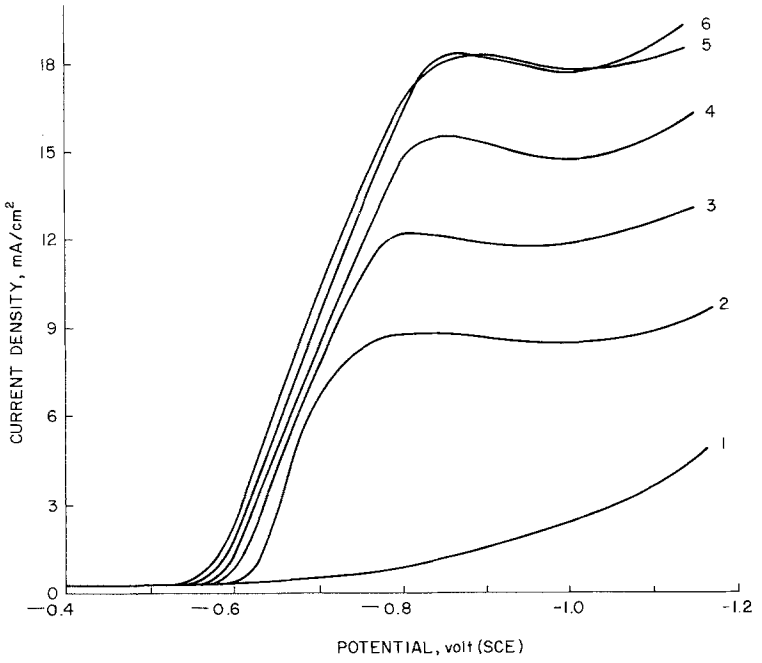

Fig. 8. Concentration effects of the lead additive on the Cr^{2+}/Cr^{3+} redox reaction on a graphite cloth electrode; sweep rate 0.5 mV s^{-1}. Electrolyte 1 mol dm^{-3} HCl + 0.1 mol dm^{-3} Cr^{3+}. The Pb^{2+} concentrations are: (1) 0.0 mol dm^{-3}; (2) 2.4×10^{-5} mol dm^{-3}; (3) 3.6×10^{-5} mol dm^{-3} (4) 4.8×10^{-5} mol dm^{-3}; (5) 6×10^{-5} mol dm^{-3}; (6) 7.2×10^{-5} mol dm^{-3}.

H_2 evolution. The lead deposition and dissolution peaks in this study are roughly symmetric about − 0.6 V (SCE). This should be compared with − 0.375 V (SCE) for the standard potential of the redox couple Pb^{2+}/Pb. Monolayer underpotential deposition of lead on the basal planes of stress-annealed pyrolytic graphite has been reported [11]. However, it is generally recognized that metal deposition from aqueous solution on to graphite is accompanied by a significant nucleation overpotential [12].

In order to determine the effect of lead concentration, a series of linear sweep voltammograms with increasing Pb^{2+} concentration were recorded as shown in Fig. 8. It shows that the limiting current of Cr^{3+} reduction increases with an increase in Pb^{2+} concentration and reaches a saturation point at about 6×10^{-5} mol dm^{-3} Pb^{2+}. The volume of the solution was 250 cm^3 and the electrochemically active surface area was about 150 cm^2 (10 cm^2 the geometric area, with a porous factor of 15). Assuming that all the lead ions in the solution are deposited onto the electrode surface and that the C–C interatomic distance is 1.5 Å, one obtains an estimated surface lead concentration of 10 monolayers. This may suggest that lead deposition forms islands on the electrode surface and that it takes about 10 monolayers of lead to fully cover the electrode.

3.6. *Electrochemically produced chromous ions*

In the studies reported above, the electrolyte solutions were started primarily with chromic ions. Chromous ions are unstable and can be readily oxidized to chromic ions by exposure to air [13]. In order to study electrode activities with respect to the Cr^{2+} oxidation reaction, it is necessary to use solutions with a significant Cr^{2+} concentration. Chemically produced Cr^{2+} solutions have been reported by dissolving metallic chromium in acid [14] or by reducing Cr^{3+} with zinc metal [15]. Electrochemically, Cr^{2+} cannot be easily produced in an ordinary one-compartment cell. This is because the Cr^{2+} produced on the working electrode would migrate and be oxidized back to Cr^{3+} on the counter-electrode.

However, chromous-rich solution can be produced electrochemically in a cell consisting of two compartments separated by an ion-selective (anion permeable, e.g. Ionics CDIL) membrane. The starting solutions are similar to those in a Redox Flow Cell [1] with Cr^{3+} in the working electrode compartment and Fe^{2+} in the counter-electrode compartment. A reversible redox couple such as Fe^{3+}/Fe^{2+} in the counter electrode compartment is desirable since Cl_2 is produced if the supporting electrolyte (HCl) is the only constituent in this compartment. The cross-mixing of Fe^{2+} and

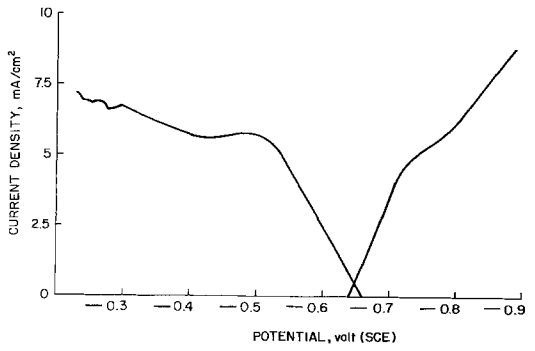

Fig. 9. Linear sweep voltammogram of a ZrC electrode in an electrolyte of 1 mol dm^{-3} HCl + 0.05 mol dm^{-3} Cr^{3+} + 0.05 mol dm^{-3} Cr^{2+}.

Cr^{3+} is minimal and it can be further eliminated by using two membranes and cycling the solution (only HCl) in the new compartment established between the two membranes. A chromous-rich solution can thus be produced by maintaining the working electrode at −0.75 V (SCE). The concentration of Cr^{2+} can be monitored easily by an ampere-hour meter.

Figure 9 shows linear sweep voltammograms of an activated ZrC electrode in a solution of approximately equal Cr^{2+} and Cr^{3+} concentration. Again the solution was gently stirred and the results showed limiting currents in both anodic and cathodic directions. The limiting currents are rather symmetric (except beyond − 0.8 V vs SCE when H_2 evolution occurs) and they are at least one order of magnitude greater than those on a carbon electrode.

3.7. *Complex formation of Cr^{3+}/Cr^{2+}*

Chromic and chromous ions exist in aqueous solutions as $Cr(H_2O)_6^{3+}$ and $Cr(H_2O)_6^{2+}$, respectively. Aqua complexed Cr^{2+} is labile and can exchange water with various ions in its inner coordination sphere while aqua complexed Cr^{3+} is not labile [9]. With negative ions (e.g. Cl^-, Br^-) in the solution and adsorbed on the electrode surface, the following chemical reaction can occur prior to the charge transfer:

$$Cr(H_2O)_6^{2+} + X_{ad}^- \rightleftarrows [Cr(H_2O)_5X]^+ + H_2O. \quad (4)$$

Therefore, depending on whether Cr^{2+} is inner-sphere coordinated or not, the following two charge transfer reactions can occur:

$$Cr(H_2O)_6^{2+} + X_{ad}^- \overset{k_1}{\rightleftarrows} [Cr(H_2O)_5X]^{2+} + e + H_2O \quad (5)$$

or

$$Cr(H_2O)_6^{2+} \overset{k_2}{\rightleftarrows} Cr(H_2O)_6^{3+} + e. \quad (6)$$

The rate constant k_1 may be greater than k_2 if the negative ions in the inner coordination sphere facilitate the charge transfer process. Donovan and Yeager [9] studied the effects of Cl^- on the Cr^{3+}/Cr^{2+} redox reaction on mercury. Some of their results are reproduced in Fig. 10 for comparison. Curve A in Fig. 10a is the initial sweep of $Cr(H_2O)_6^{3+}$ in $NaClO_4$ which is an inert supporting electrolyte and curve B is the initial sweep with a small amount of Cl^- in the solution. The cathodic peaks of these two curves are similar since the only reaction is the reduction of $Cr(H_2O)_6^{3+}$ (reverse reaction of Equation 6). The anodic peak of curve A is simply the oxidation of $Cr(H_2O)_6^{2+}$ (forward reaction of Equation 6). However, the anodic peak of curve B corresponds to the oxidation of both $Cr(H_2O)_6^{2+}$ and $[Cr(H_2O)_5Cl]^+$ (forward reactions of Equations 6 and 5). This is because after the initial cathodic sweep, inner-sphere coordinated $[Cr(H_2O)_5Cl]^+$ ions become available for oxidation in a Cl^- containing electrolyte. It was found that the double-layer corrected rate constant k_1 (Equation 5) is about two orders of magnitude greater than k_2 (Equation 6) [9]. Therefore, it is desirable to use electrodes which could accomodate the substitution of one inner-sphere water molecule of Cr^{2+} by a negative ion such as Cl^-. However, it should also be pointed out that the standard potential of the redox couple $[Cr(H_2O)_6]Cl^+/[Cr(H_2O)_5Cl]^{2+}$ is at least 100 mV (also Cl^- concentration dependent, see Donovan and Yeager [9]) positive to that of the redox couple $[Cr(H_2O)]_6^{2+}/[Cr(H_2O)_6]^{3+}$. This would reduce the open circuit potential by a similar amount in a Redox Flow Cell.

Most cyclic voltammograms of similar sweep rate in this study (e.g. Figs. 1 and 3) seem to indicate that the only redox couple involved in the reaction was $Cr(H_2O)_6^{2+}/Cr(H_2O)_6^{3+}$ even though there were plenty of chloride ions in the electrolyte. However, at times voltammograms such as shown in Fig. 10b were obtained. The dotted curve is the fifth sweep and the solid curve is a

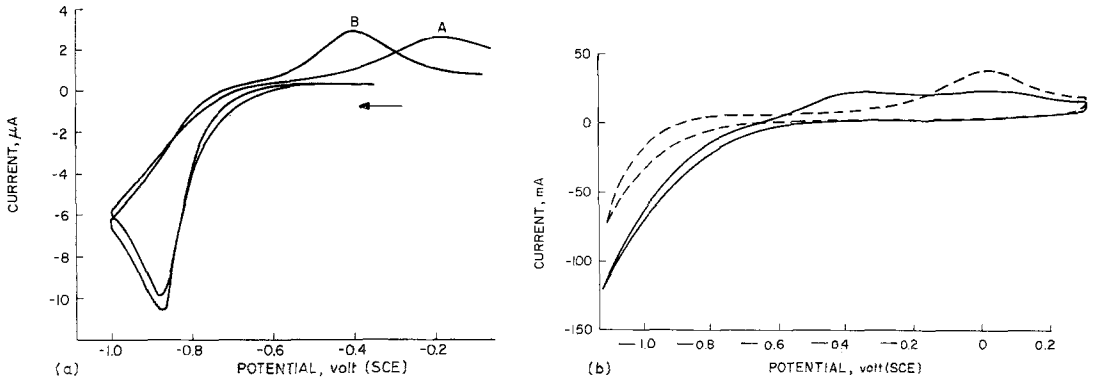

Fig. 10. The effects of inner sphere coordination of chloride ions with chromium ions. (a) Initial scans for Cr^{3+} reduction on a hanging mercury electrode, sweep rate 110 mV s^{-1}; curve A solution contains no Cl^-. Curve B contains 5 × 10^{-3} mol dm^{-3} Cl^- (from [6]). (b) Voltammograms of a carbon electrode in 1 mol dm^{-3} HCl + 0.005 mol dm^{-3} Cr^{3+}. Sweep rate 140 mV s^{-1}. Dotted curve, 5th cycle; solid curve, 50th cycle.

scan after 50 cycles. This solid curve can be compared with Fig. 10a and suggests the existence of the redox reaction $[Cr(H_2O)_5Cl]^{2+}/[Cr(H_2O)_6]Cl^+$.

The substitution of one of the inner-sphere water molecules of Cr^{2+} by a negative ion involves a precursor step of anion specific adsorption on the electrode. Since specific adsorption is closely related to the potential of zero charge (PZC) of a particular electrode surface, one can speculate that the PZC of graphite cloth is not favourable for Cl^- adsorption under the general conditions of this study. The graphite surface is notorious for its electrochemical non-reproducibility [16], and it is conceivable that under certain conditions (e.g. impure solution) the PZC will shift and favour significant Cl^- adsorption and the subsequent inner-sphere substitution. It is obvious that $[Cr(H_2O)_5Cl]^{2+}/[Cr(H_2O)_6]Cl^+$ is a much more reversible redox couple than $Cr(H_2O)_6^{3+}/Cr(H_2O)_6^{2+}$. Therefore, electrode materials with good Cl^- adsorption characteristics in the potential region down to − 0.85 V (SCE) is desirable for the development of the Redox Flow Cell.

4. Conclusions

It has been shown that the simple evaluation procedures adopted here can provide useful information about the characteristics of porous electrodes for the Cr^{3+}/Cr^{2+} redox reaction. The favourable performance of ZrC is encouraging and leads one to speculate on a whole class of materials, namely, the transition metal carbides and nitrides. These materials are chemically stable and mechanically strong. Since one can conveniently control the composition ratio and impurity levels, one has the freedom to modify the electronic structure of these materials (e.g. adjust the Fermi level, vary the conductivity, etc.) and to facilitate electron transfer to and from chromium ions.

Lead chloride has been proven to be a catalytic additive with good selectivity. The lead layers formed on the electrode surface not only increase the Cr^{3+} reduction rate but also decrease the H_2 evolution reaction. Methods for improving the bonding and uniformity of lead on the surface are currently being studied at the NASA Lewis Research Center [15].

Most systems studied in this report are not well-defined for rigorous kinetic analysis, i.e. porous electrodes with poorly controlled mass transport. Nevertheless, it is shown that simple voltammetric expressions can be applied to estimate certain kinetic parameters. In order to obtain definitive kinetic data for these electrode materials, one should apply rotating ring disc techniques to non-porous electrodes. Finally, further studies on the electronic structure of these systems are needed.

Acknowledgements

The author received a Research Associateship (1977–1978) from the National Research Council and the work was carried out at the NASA Lewis Research Center. The author would like to thank L. Thaller, R. Post, R. Gahn, D. Lauver and J. Ferrante at Lewis for their technical assistance. He also appreciates several useful discussions with

E. Yeager at Case Western Reserve University.

References

[1] L. H. Thaller, NASA Technical Report TMX-71540 (1974).
[2] A. R. Driesner, E. K. Storms, P. Wagner and T. C. Wallace, *Proceedings of the Chemical Vapor Depositon, Fourth International Conference,* (edited by G. F. Wakefield and T. M. Blocher Jr) Electrochemical Society, Princeton (1973) p. 473.
[3] E. G. Gagnon, *J. Electrochem. Soc.* **122** (1975) 521.
[4] H. N. Seiger, NASA Technical Report Cr-132481 (1975).
[5] J. P. Randin and E. Yeager, *J. Electrochem. Soc.* **36** (1972) 257.
[6] J. P. Randin and E. Yeager, *J. Electrochem. Soc.* **58** (1975) 313.
[7] P. Delahay, 'New Instrumental Methods in Electrochemistry', Interscience Publisher, New York, (1954) Chap. 6.
[8] E. Gileadi, E. Kirowa-Eisner and J. Penciner, 'Interfacial Electrochemistry', Addison-Wesley, Memlo Park (1975) p. 370.
[9] S. S. Donovan and E. Yeager, Techincal Report No. 24, Electrochemistry Research Lab., Case Western Reserve University (1969).
[10] J. Giner and K. Cahill, NASA Technical Report CR-159738 (1980).
[11] I. Marcos, *J. Electroanal. Chem.* **66** (1975) 250.
[12] M. Fleischmann and H. R. Thirsk, 'Advances in Electrochemistry and Electrochemical Engineering' Vol. III, (edited by P. Delahay and C. W. Tobias) Wiley, New York, (1963) Ch. 3.
[13] M. Ardon and R. Plane, *J. Amer. Chem. Soc.* **81** (1959) 3197.
[14] H. Lux and G. Illmann, *Ber. der Deutch Chem. Gesell.* **91** (1958) 2143.
[15] V. S. Srinivasan, G. Torsi and P. Delahay, *J. Electroanal. Chem.* **10** (1965) 165.
[16] R. E. Panzer and P. J. Elving, *Electrochimic Acta* **20** (1975) 635.
[17] J. Giner and K. Cahill, US Patent 4, 192, 910 (1980).